Journal of Inclusion Phenomena and Macrocyclic Chemistry (2024) 104:501–512
https://doi.org/10.1007/s10847-024-01250-4

ORIGINAL ARTICLE

Encapsulation investigation of molnupiravir drug guest using cucurbituril hosts through the DFT approach

Wandee Rakrai[1] · Butsayamat Rattanadon[1] · Chanukorn Tabtimsai[1] · Chatthai Kaewtong[2] · Banchob Wanno[2]

Received: 25 April 2024 / Accepted: 12 June 2024 / Published online: 2 July 2024

Abstract

The geometrical structures of cucurbit[*n*]uril (CB[*n*], *n* = 5–8 and their complexes with molnupiravir (MLP) drug have been investigated using the DFT computations. The complexation energies and electronic properties of CB[*n*]/MLP complexes were also computed. The host–guest interactions in the complexation are occurred through the of dipole–dipole interactions which are the hydrogen bonds between the O−H or N−H of molnupiravir and oxygen atoms of CB[*n*]s. The CB[*n*]/MLP host–guest complexation in both gas and water are found to be an exothermic reaction with negative complexation energy values. By means of the NBO analysis and MEP contours, the partial charge transfers from CB[*n*]s to molnupiravir are displayed. After drug complexation, the electronics properties of CB[*n*]s are significantly changed. This means that CB[*n*]s can act as a host for appropriately molnupiravir guest, even in aqueous solution.

Keywords Cucurbit[*n*]uril · DFT · Drug delivery · Host–guest complex · Molnupiravir

Introduction

The molnupiravir (MLP) has been known to be a pro-drug of the nucleoside analogue N^4-hydroxycytidine and an antiviral drug used for the influenza treatment [1, 2]. In addition, it has recently been known as an oral antiviral treatment drug of COVID-19 [3]. Molnupiravir reduces the virus's ability to replicate, by this means slowing the disease. The clinical trials show a meaningfully lower risk of hospitalization in adults experiencing mild COVID-19 [4]. However, molnupiravir has some side effects like any other drug, such as diarrhea, nausea, and dizziness [5]. Most therapeutic COVID-19 drugs have been discarded due to their low efficiency due to several factors, such as poor solubility and drug release and other toxic effects. To solve these factors, a drug delivery system via host–guest formation based on the encapsulation of a guest (drug of interest) molecule inside the cavity of a macrocyclic host by noncovalent interaction and bonding has been developed [6, 7]. The noncovalent interactions of host–guest formation include van der Waals force, π–π stacking interaction, hydrogen-bonding, electrostatic interaction, and hydrophobic/hydrophilic interaction [8, 9]. In particular, hydrogen bond is a noncovalent interaction that stabilize the formed complexes [10].

Cucurbiturils or cucurbit[n]urils (CB[*n*]s) are one of the major macrocyclic hosts for drug delivery vehicles due to their comparatively low toxicity and ability to make guest compound crossing via the cellular membrane easier [11, 12]. The molecular formula of CB[*n*]s is $C_{6n}H_{6n}N_{4n}O_{2n}$, which has a simple structure with a pumpkin-like geometry [13, 14]. The main characteristic of macrocyclic hosts is their hydrophobic cavity interior with hydrophilic exteriors that allow them to afford partial or complete encapsulation of drugs through noncovalent interactions such as ion–dipole interactions and hydrogen bonding interaction between macrocyclic host and drug [15–18]. However, because experimental method is expensive and time-consuming, there is more advantageous to model them theoretically before successful experimental studies. The density functional theory (DFT) computation is a powerful theoretical tool which is applied for studying the host–guest interaction between

✉ Banchob Wanno
banchobw@gmail.com

[1] Computational Chemistry Center for Nanotechnology and Department of Chemistry, Faculty of Science and Technology, Rajabhat Maha Sarakham University, Maha Sarakham 44000, Thailand

[2] Nanotechnology Research Unit and Supramolecular Chemistry Research Unit, Department of Chemistry and Center of Excellence for Innovation in Chemistry, Faculty of Science, Mahasarakham University, Maha Sarakham 44150, Thailand

drugs and macrocyclic hosts such as calix[*n*]arenes, cyclodextrins, and CB[*n*]s. The DFT method was performed for theoretical modeling on the interactions between the CB[*n*]s and drugs such as fluorouracil [19], capecitabine [20], oseltamivir [21], and gemcitabine [22].

To our recent knowledge, there has not been reported of a systematic theoretical investigation of the complexation between molnupiravir and CB[*n*]s. So, in the present work, a systematic theoretical investigation of the host–guest complexations between molnupiravir and cucurbit[*n*]uril (*n* = 5–8) and their energetical and geometrical properties by means of the DFT calculations has been investigated. Moreover, the electronic properties such as charge transfer, energies of the highest occupied molecular orbital (HOMO), the lowest unoccupied molecular orbital (LUMO), and molecular electrostatic potential (MEP) for the species and complexes have been also computed and reported.

Computational details

The initial geometries of cucurbit[*n*]urils (CB[*n* = 6–8]) have been adopted from previously reported [21]. The optimized structures of molnupiravir (MLP), CB[*n*] (*n* = 5–8) and their complexes were performed at the density functional calculations. All calculations were carried out with the Becke three-parameters exchange functionals and LYP correlation functional (B3LYP) theory. The 6–31G(d,p) basis set was used [23–25]. The geometrical structures of the MLP and CB[*n*] molecules have been optimized prior to forming the 1:1 host–guest supramolecular assemblies. By means of the corresponding optimized structures of MLP and CB[*n*] compounds, the assemblies have been constructed as displayed in Fig. 1. The model in which MLP entering into the CB[*n*] cavity by isopropyl was named the MLP–1 complex, the other in which MLP entering into the CB[*n*] cavity by aromatic group was named the MLP–2 complex. Full geometrical optimizations of the MLP, CB[*n*]s and their complexation structures without any geometrical or symmetry constrains have been performed. So, the MLP compound had to move in the CB[*n*] cavity during the whole optimization process. The highest occupied molecular orbital (E_{HOMO}) and the lowest unoccupied molecular orbital (E_{LUMO}) energies have been also calculated.

All calculations were carried out using the GAUSSIAN 09 program package [26]. Electronic properties of all species were computed in the gas and water phases. The computations in water phase, the solvent effect under the conductor–like polarizable continuum model (CPCM) [27, 28] have been carried out. To understand the complexation stability, the complexation energy (E_{cpx}) between CB[*n*] and molnupiravir was calculated according to the following equation:

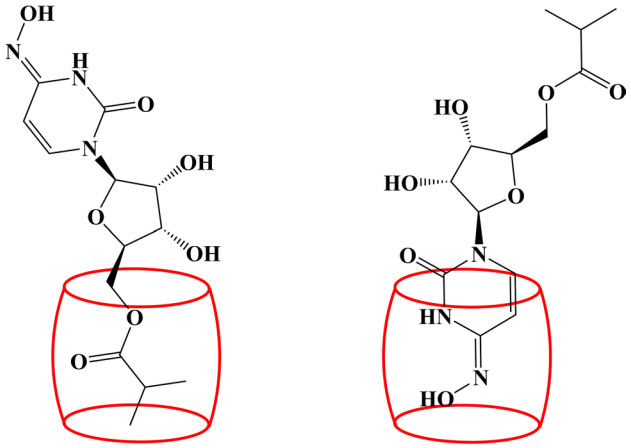

Fig. 1 Schematics of the 1:1 molecular host–guest supramolecular assemblies of MLP with CB[*n*]

$$E_{cpx} = E_{H-G} - \left(E_H + E_G\right) \quad (1)$$

where $E_{\mathrm{H\text{-}G}}$, E_{H} and E_{G} are the total energy of the complex, the free optimized CB[*n*], and the free optimized molnupiravir energy, respectively.

The natural bond orbital (NBO) were performed as implemented in GAUSSIAN 09 program. The partial charge transfers (PCTs) during complexation were defined as a change in molnupiravir charges during the complexation using the calculated natural bond orbital charges. Finally, the molecular graphics and electrostatic potential of studied compound were generated with MOLEKEL 4.3 program [29].

Results and discussion

Geometrical structures

The geometrical structures of molnupiravir, cucurbit[*n*]uril (n = 5–8) and their complexes with molnupiravir were computed by full optimization without any constrains using the DFT computation. Fully optimized geometries of molnupiravir and free cucurbit[*n*]uril molecules are displayed in Figs.2, 3, respectively. The optimized geometrical structure of CB[5] is found to possess as a D_{nh} symmetrical structure. The intramolecular depths of the CB[5] cavity is 6.23 Å. The intermolecular distance between the oxygen portals for CB[5] is 5.46 Å. While, the geometrical structures including the symmetrical structure, the intramolecular depths of the cavity and the intermolecular distances between the oxygen portals of CB[6]–CB[8] are according to the earlier computed values [21].

To examine the possible geometries of the CB[*n*]/MLP complexes, two types of the possible 1:1 molecular host–guest inclusion modes of binding motive via

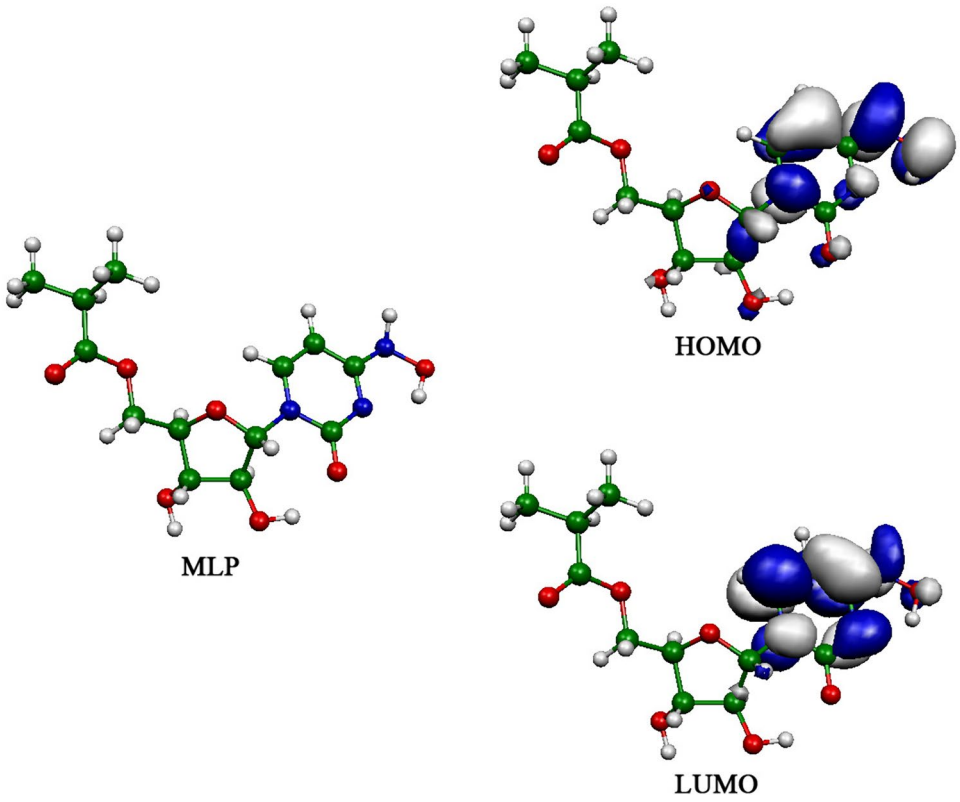

Fig. 2 Optimized structure, HOMO and LUMO of molnupiravir

isopropyl (CB[*n*]/MLP–1) and aromatic (CB[*n*]/MLP–2) side chains of MLP pointing to CB[*n*] cavities are obtained (Fig. 1). The DFT optimized structures of molnupiravir complexes with the CB[5]–CB[8] are displayed in Figs. 4, 5. The optimized structures for all CB[*n*]/MLP complexes present that most of molnupiravir is still positioned inside the CB[6]–CB[8] cavities except for CB[5]/MLP complex, molnupiravir is expelled out of CB[5]. This imply that the CB[5] cavity size is too small for molnupiravir inclusion. Upon inclusion of MLP drug, the CB[*n*] diameter undertakes a change with extension in one direction, while the other side undertakes a contraction. After MLP inclusion into CB[*n*]s, it is found that there is not remarkable change in the geometric structure of MLP.

The calculated results also show that the CB[*n*] can form stable complexes with molnupiravir through dipole–dipole interactions such as the hydrogen bonds between the O−H or N−H of molnupiravir drug and portal oxygen atoms of CB[*n*]. The number of hydrogen bonds and average hydrogen bond distances of CB[5]–CB[8] complexes with MLP drug with different inclusion orientations are listed in Table 1. It is found that, all CB[*n*] can form the stable complexes with MLP through hydrogen bonds, except for CB[5]/MLP–1 and CB[6]/MLP–1 complexes. The average hydrogen bond distances of CB[*n*]/MLP complexes are found in the range of 2.036–2.282 Å.

Complexation energies

To know the complexation ability, the complexation energies (E_{cpx}) of the MLP with CB[*n*] were computed. The complexation energy was defined as the energy difference between the total energy of CB[*n*]/MLP complex and the total energy of the free CB[*n*] and MLP compound at their most stable geometry. The complexation energies of the CB[5]–CB[8] with molnupiravir in gas and water phases computed at the B3LYP/6–31G(d,p) theoretical level are listed in Table 1. The negative complexation energy values reveal that the inclusion complexes are exothermic process. The complexation energies of all complexes in gas phase are found to be in the range of − 6.02 to − 19.66 kcal/mol. The complexation energy of CB[8]/MLP–2 complex show the most energetically favorable value of − 19.66 kcal/mol. The complexation abilities of CB[*n*] to molnupiravir drug in gas phase are in the order: CB[8]/MLP–2 (− 19.66 kcal/mol) ≈ CB[7]/MLP–1 (− 19.45 kcal/mol) > CB[8]/MLP–1 (− 18.47 kcal/mol) > CB[7]/MLP–2 (− 17.39 kcal/mol) > CB[5]/MLP–1 (− 15.97 kcal/mol) > CB[5]/MLP–2 (− 13.49 kcal/mol) > CB[6]/MLP–1 (− 8.12 kcal/mol) > CB[6]/MLP–2 (− 6.02 kcal/mol), respectively. It is found that, CB[8]/MLP–2 complex has the most energetically favorable value among the other complexes which corresponds to a large number

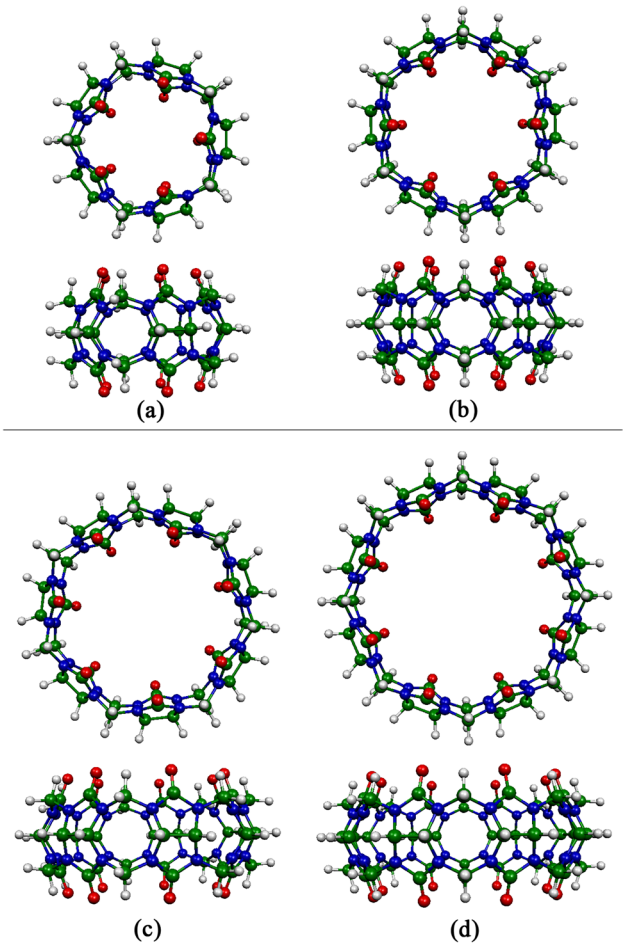

Fig. 3 Optimized structures of **a** CB[5], **b** CB[6], **c** CB[7], and **d** CB[8]

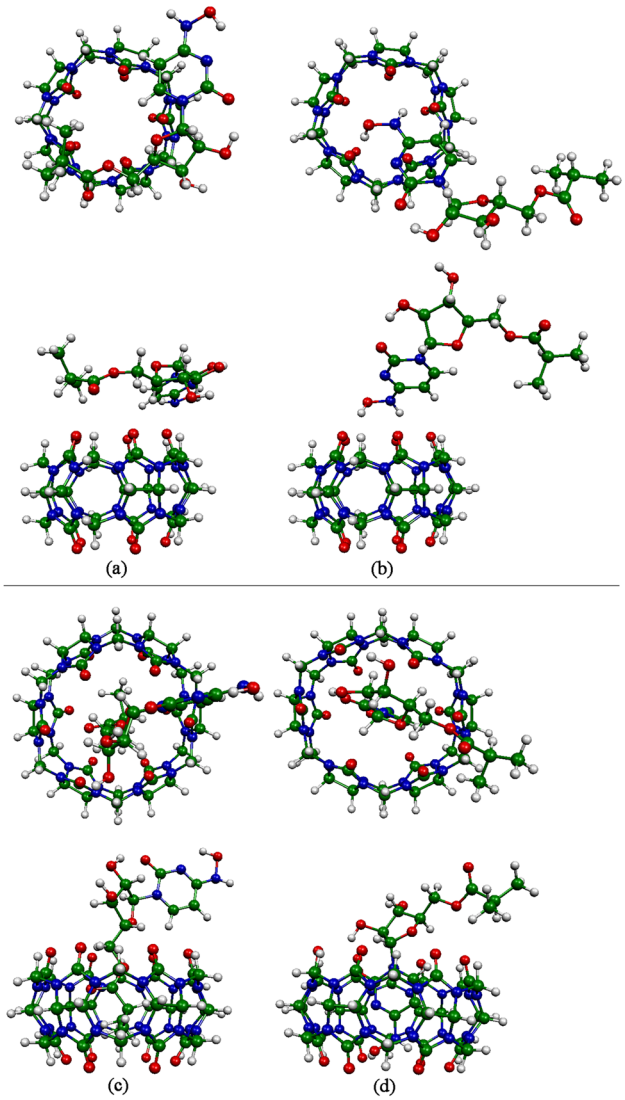

Fig. 4 Optimized structures of **a** CB[5]/MLP–1, **b** CB[5]/MLP–2, **c** CB[6]/MLP–1, and **d** CB[6]/MLP–2 complexes. Birds eye–view (top) and side view (bottom)

of hydrogen bonds and short average hydrogen bond distance compared to CB[7]/MLP–2 with the same number of hydrogen bonds. In addition, the hydrogen bonds of CB[8]/MLP–2 complex are more stronger than hydrogen bonds of CB[7]/MLP–2 complex according to the differences in their bond angles in which the hydrogen bond angles of CB[8]/MLP–2 complex are more close to 180 degrees than that of the CB[7]/MLP–2 complex.

In water phase, the complexation energies of all complexes are negative values except for CB[6]/MLP complexes. The complexation energies of all complexes in water phase are in the range of − 4.39 to − 12.80 kcal/mol. This indicates that complexations are also processed via exothermic reaction and all complexes are also stable in water phase as same as in the gas phase, except for CB[6]/MLP complexes. In the gas phase, the complexation energies are very high compared to the water phase. The higher values of complexation energies in the gas phase ascend as the water molecules in the CB[*n*] cavity are not considered in the gas phase computations. Whereas in the water phase, those water molecules can bind with MLP and CB[*n*]s via hydrogen bonding interaction and stabilize the complexes [30–32].

Charge and electronic properties

Upon the complexation of molnupiravir drug with CB[*n*]s, the effects of molnupiravir drug on CB[*n*] electronic behavior have been investigated to explore their electronic structural change. In addition, the chemical activity of CB[*n*]s to molnupiravir, the highest occupied molecular orbital (HOMO), the lowest unoccupied molecular orbital (LUMO), and energy gap (E_{gap}) have been computed. The energy gap is defined as the gap between HOMO and LUMO energies. The electronic properties of the CB[*n*]s comparing with their complexes with molnupiravir were

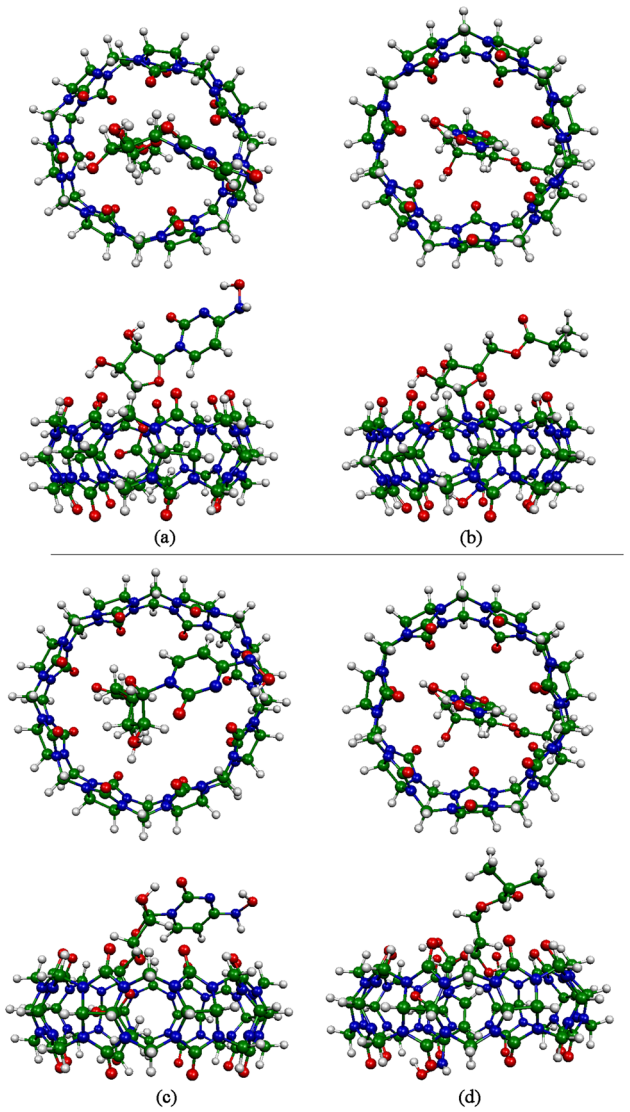

Fig. 5 Optimized structures of **a** CB[7]/MLP–1, **b** CB[7]/MLP–2, **c** CB[8]/MLP–1, and **d** CB[8]/MLP–2 complexes. Birds eye–view (top) and side view (bottom)

used to evaluate the chemical activity of CB[*n*]s. The computed HOMO and LUMO energies and energy gaps of CB[*n*]s and theirs complexes with molnupiravir drug computed in both gas and water phases are listed in Table 2. In the gas phase, the results display that the HOMO levels of CB[*n*]s are not remarkably different from that of MLP, nevertheless the LUMO levels of CB[*n*]s are higher than that of MLP. This means that in CB[*n*]/MLP complexes, electron can transfer from CB[*n*]s to MLP. The energy gaps of CB[5], CB[6], CB[7], and CB[8] are computed to be 7.196, 7.228, 7.237, and 7.224 eV, respectively, these results are found to be in good agreement with the previous works [21]. For the CB[*n*]/MLP complexes, the energy gaps of CB[*n*]/MLP complexes are found in the range of

Table 1 The complexation energies (E_{cpx}) in gas and water phases (in parenthesis) and partial charge transfers (PCTs), average hydrogen bond distance (HBD), and number of hydrogen bond (HB) of CB[*n*]/MLP complexes obtained from the B3LYP/6–31G(d,p) theoretical level

Complexes	E_{cpx} [a]	PCT[b]	Average HBD[c]	Number of HB
CB[5]/MLP–1	− 15.97 (− 4.39)	− 0.004	–	–
CB[5]/MLP–2	− 13.49 (− 8.65)	− 0.026	2.177	2
CB[6]/MLP–1	− 8.12 (–[d])	− 0.038	–	–
CB[6]/MLP–2	− 6.02 (–[d])	− 0.057	2.249	3
CB[7]/MLP–1	− 19.45 (− 12.20)	− 0.043	2.036	1
CB[7]/MLP–2	− 17.39 (− 12.50)	− 0.057	2.282	4
CB[8]/MLP–1	− 18.47 (− 9.89)	− 0.049	2.057	2
CB[8]/MLP–2	− 19.66 (− 12.80)	− 0.055	2.188	4

[a]In kilocalories/mol (kcal/mol)

[b]In electrons (*e*)

[c]In angstroms

[d]unconvergence

4.956–5.426 eV. In the water phase, the calculated results display that the HOMO levels of CB[*n*]s are also slightly different from that of MLP, nevertheless the LUMO levels of CB[*n*]s are also found to be higher than that of MLP. This means that in CB[*n*]/MLP complexes, electron can transfer from CB[*n*]s to MLP. The energy gaps of CB[5], CB[6], CB[7], and CB[8] are computed to be 7.184, 7.320, 7.347, and 7.374 eV, respectively. For the CB[*n*]/MLP complexes, the energy gaps of CB[*n*]/MLP complexes are computed to be in the range of 5.089–5.442 eV. These deceasing of energy gaps of CB[*n*]s which appears after complexation with molnupiravir drug in both gas and water phases may be due to the electrons are transferred from CB[*n*]s to molnupiravir drug which confirmed by the charge transfer analysis. Moreover, the results indicate that all of CB[*n*]s are changed in their electrical conductivities due to molnupiravir complexation. The dipole moment of MLP is larger than that of CB[*n*]s, which implies that inclusion of MLP into CB[*n*] can modify the dipole moment of MLP. Most of dipole moments of CB[*n*]/MLP complexes are found to be larger than MLP, this implies that CB[*n*]/MLP complexes can have more solubility in water than free MLP.

In addition, the quantum molecular descriptors i.e., electronic chemical potential (μ), electronegativity (χ), chemical hardness (η), electrophilicity (ω), and chemical softness (S) of the CB[*n*] and their complexation with molnupiravir drug were computed and analyzed (Table 2). They were calculated from the HOMO and LUMO energy levels (Eq. (2)–(6)). The μ, χ, η, ω, and S are considered as the first and the second partial derivatives of electronic energy (E) with respect to the number of electrons (N) at a fixed external potential

Table 2 The highest occupied molecular orbital energies (E_{HOMO}, eV), the lowest unoccupied molecular orbital energies (E_{LUMO}, eV), energy gaps (E_{gap}, eV), electronic chemical potential (μ, eV), electronegativity (χ, eV), chemical hardness (η, eV), electrophilicity (ω, eV), and softness (S, eV) of molnupiravir, CB[n] and CB[n]/MLP complexes obtained in gas and water phases (in parenthesis)

Type	E_{HOMO}	E_{LUMO}	E_{gap}	μ	χ	η	ω	S
MLP	− 6.328	− 1.299	5.030	− 3.813	3.813	2.515	2.891	0.199
	(− 6.204)	(− 1.088)	(5.116)	(− 3.646)	(3.646)	(2.558)	(2.599)	(0.195)
CB[5]	− 6.377	0.819	7.196	− 2.779	2.779	3.598	1.073	0.139
	(− 6.613)	(0.571)	(7.184)	(− 3.021)	(3.021)	(3.592)	(1.270)	(0.139)
CB[6]	− 6.424	0.803	7.228	− 2.811	2.811	3.614	1.093	0.138
	(− 6.694)	(0.626)	(7.320)	(− 3.034)	(3.034)	(3.660)	(1.258)	(0.137)
CB[7]	− 6.507	0.730	7.237	− 2.888	2.888	3.619	1.153	0.138
	(− 6.749)	(0.599)	(7.347)	(− 3.075)	(3.075)	(3.674)	(1.287)	(0.136)
CB[8]	− 6.574	0.649	7.224	− 2.963	2.963	3.612	1.215	0.138
	(− 6.803)	(0.571)	(7.374)	(− 3.116)	(3.116)	(3.687)	(1.316)	(0.136)
CB[5]/MLP−1	− 5.804	− 0.708	5.095	− 3.256	3.256	2.548	2.081	0.196
	(− 6.150)	(− 1.061)	(5.089)	(− 3.606)	(3.606)	(2.544)	(2.555)	(0.197)
CB[5]/MLP−2	− 5.261	0.164	5.426	− 2.548	2.548	2.713	1.197	0.184
	(− 6.095)	(− 0.653)	(5.442)	(− 3.374)	(3.374)	(2.721)	(2.092)	(0.184)
CB[6]/MLP−1	− 5.489	− 0.362	5.127	− 2.925	2.925	2.564	1.669	0.195
	(− 6.123)	(− 1.007)	(5.116)	(− 3.565)	(3.565)	(2.558)	(2.484)	(0.195)
CB[6]/MLP−2	− 5.144	0.133	5.277	− 2.506	2.506	2.638	1.190	0.190
	(− 5.959)	(− 0.708)	(5.252)	(− 3.333)	(3.333)	(2.626)	(2.116)	(0.190)
CB[7]/MLP−1	− 5.144	− 0.015	5.129	− 2.580	2.580	2.564	1.297	0.195
	(− 6.150)	(− 1.034)	(5.116)	(− 3.592)	(3.592)	(2.558)	(2.522)	(0.195)
CB[7]/MLP−2	− 4.669	0.297	4.965	− 2.186	2.186	2.483	0.962	0.201
	(− 5.932)	(− 0.816)	(5.116)	(− 3.374)	(3.374)	(2.558)	(2.226)	(0.195)
CB[8]/MLP−1	− 4.885	0.180	5.064	− 2.352	2.352	2.532	1.093	0.197
	(− 6.095)	(− 1.007)	(5.089)	(− 3.551)	(3.551)	(2.544)	(2.478)	(0.197)
CB[8]/MLP−2	− 4.489	0.467	4.956	− 2.011	2.011	2.478	0.816	0.202
	(− 5.932)	(− 0.844)	(5.089)	(− 3.388)	(3.388)	(2.544)	(2.256)	(0.197)

(υ(r)) [33]. Base on the Janak's approximation [34], analytical and operational definitions of the quantum molecular descriptors were given as following equations:

$$\mu = \left(\frac{\partial E}{\partial N}\right)_{V\left(\vec{r}\right)} = \left(E_{LUMO} + E_{HOMO}\right)/2 \tag{2}$$

$$\chi = -\mu \tag{3}$$

$$\eta = \frac{1}{2}\left(\frac{\partial^2 E}{\partial N^2}\right)_{V\left(\vec{r}\right)} = \left(E_{LUMO} - E_{HOMO}\right)/2 \tag{4}$$

$$\omega = \frac{\mu^2}{2\eta} \tag{5}$$

$$S = \frac{1}{2\eta} \tag{6}$$

The molecular descriptors were used to describe the electron transfer between host and guest molecules and supply data about the structural stability and reactivity of all species. The increasing of the μ and η results in the decrease of the χ, ω, and S which induce the increasing of the stability and decreasing of the reactivity. The global indices of stability and reactivity in both gas and water phases are listed in Table 2. All of values of the hardness, chemical potential, electronegativity, electrophilicity, and chemical softness for complexes are modified from the individual CB[n]s and molnupiravir drug.

In gas phase, the electronic chemical potential values of all complexes are computed to be in the range of − 3.256 to − 2.011 eV. The chemical potentials of all the complexes are computed to be a negative value indicating that the inclusion complexes are in the stable form. The chemical potential can point out the affinity of electron transfer in the complexation process. The electronegativity values are computed in the range of 2.011 to 3.256 eV, and the chemical hardness values are found in range of 2.478 to 2.713 eV. The electrophilicity values are in range of 0.816 to 2.081 eV and the chemical softness values are in range of 0.184 to 0.202 eV. This indicates that after molnupiravir forms complexes with CB[n], the chemical hardness and electronegativity values of complexes are decreased, excepted the electronegativity value of CB[5]/MLP–1 and CB[6]/MLP–1 which are increased. The chemical potential and softness values are increased,

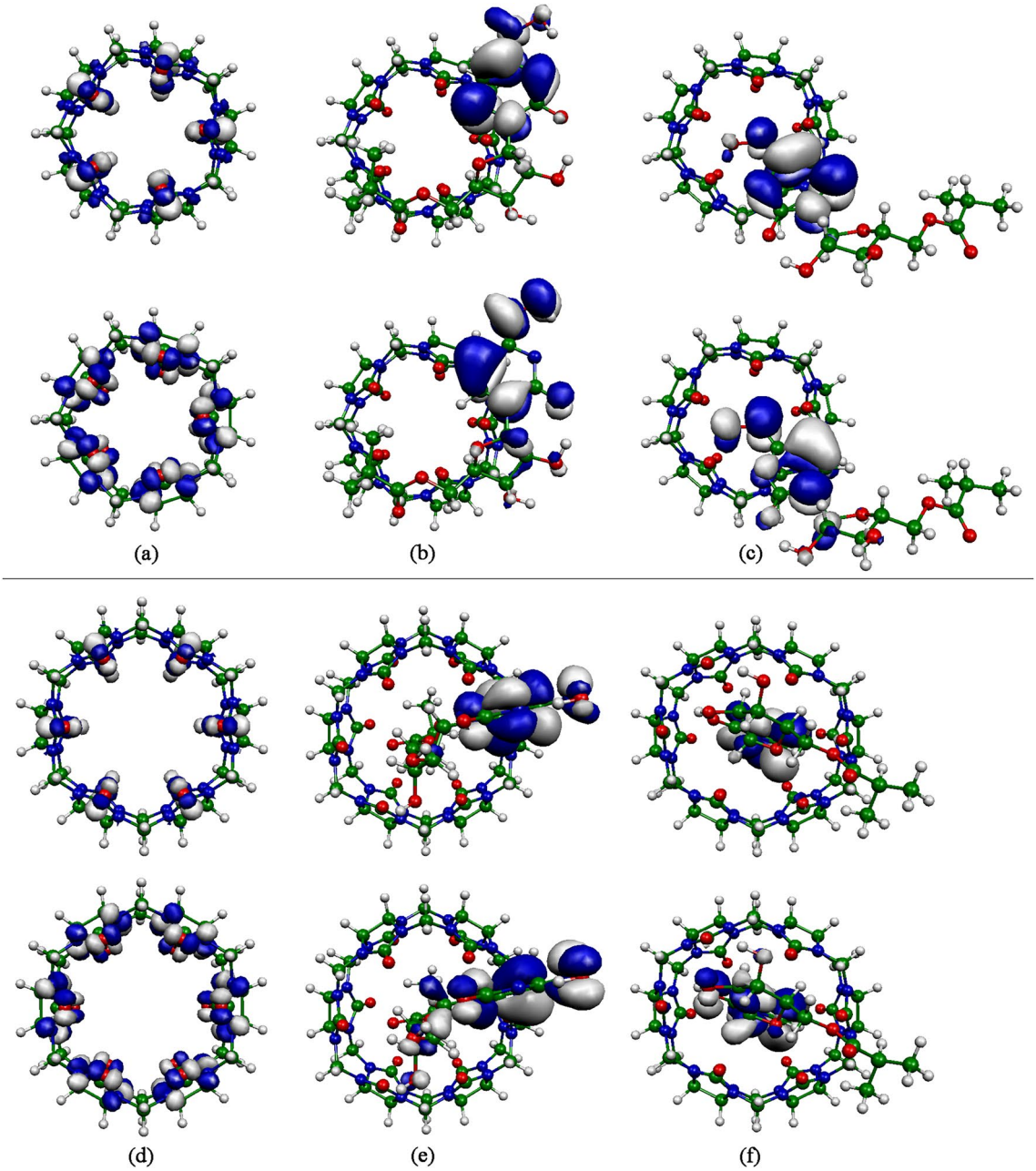

Fig. 6 Plots of the LUMO (top) and the HOMO (bottom) orbitals of **a** CB[5], **b** CB[5]/MLP–1, **c** CB[5]/MLP–2, **d** CB[6], **e** CB[6]/MLP–1, and **f** CB[6]/MLP–2

except for the chemical potential value of CB[5]/MLP–1 and CB[6]/MLP–1 are decreased. The chemical softness values of CB[*n*]/MLP complexes are higher than that of the bare CB[*n*]s, therefore the reactivity of CB[*n*]/MLP complexes is higher than that of the bare CB[*n*]s. The electrophilicity values of CB[5]/MLP complexes, CB[6]/MLP complexes and CB[7]/MLP–1 are increased while the electrophilicity values of CB[8]/MLP complexes and CB[7]/MLP–2 are decreased. Therefore, the calculated results approve that CB[*n*]s are changed in their electrical conductivity due to molnupiravir complexation.

In water phase, the electronic chemical potential and chemical hardness values of bare CB[*n*]s are in the range of − 3.116 to − 3.021 eV and 3.592 to 3.687 eV, respectively. The electronic chemical potential and chemical hardness values of CB[*n*]/MLP complexes are in the range of − 3.606 to − 3.333 eV and 2.544 to 2.721 eV, respectively. Signifying that when molnupiravir forms complexes with CB[*n*], the electronic chemical potential and chemical

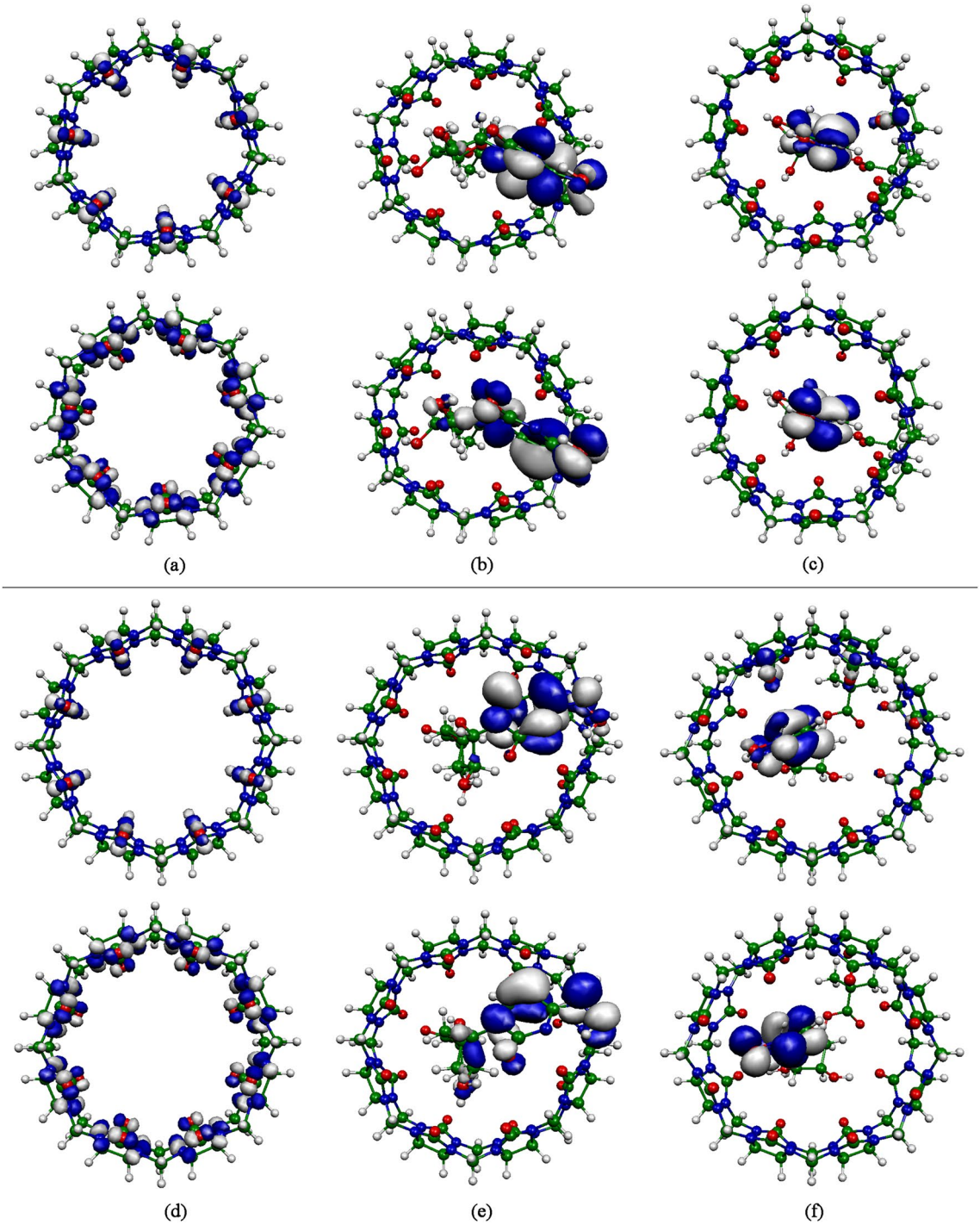

Fig. 7 Plots of the LUMO (top) and the HOMO (bottom) orbitals of **a** CB[7], **b** CB[7]/MLP–1, **c** CB[7]/MLP–2, **d** CB[8], **e** CB[8]/MLP–1, and **f** CB[8]/MLP–2

hardness values are decreased. The electronegativity, electrophilicity, and chemical softness values of bare CB[*n*]s are in range of 3.021 to 3.116 eV, 1.258 to 1.316 eV, and 0.136 to 0.139 eV, respectively. The electronegativity, electrophilicity, and chemical softness values of CB[*n*]/MLP complexes are in range of 3.333 to 3.606 eV, 2.092 to 2.555 eV, and 0.184 to 0.197 eV, respectively. This indicates that when molnupiravir forms complexes with CB[*n*], the electronegativity, electrophilicity, and chemical softness values of CB[*n*]s are increased. Therefore, the results confirm that

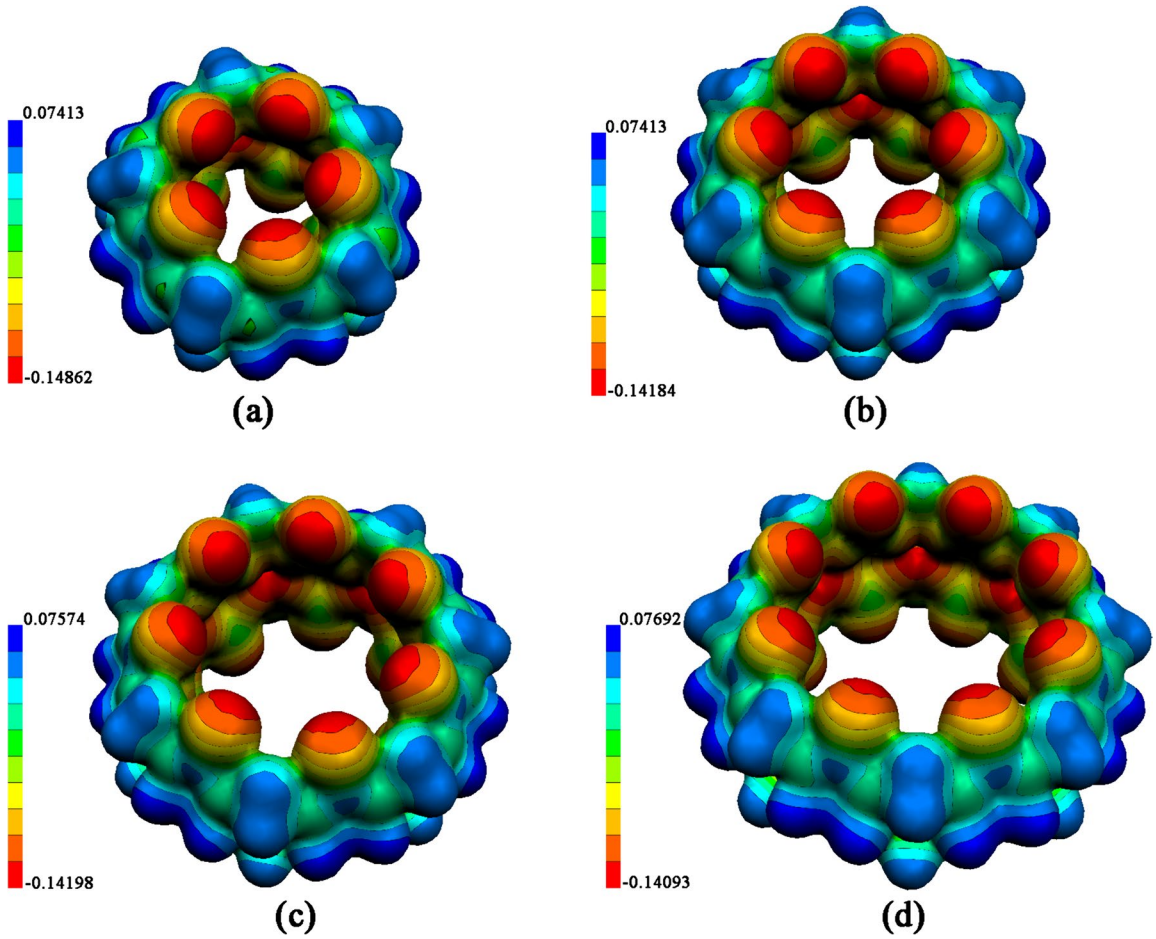

Fig. 8 Computed molecular electrostatic potentials on the molecular surfaces of **a** CB[5], **b** CB[6], **c** CB[7], and **d** CB[8]. Blue regions are more positive charges and red regions are more negative charge

after molnupiravir complexes with CB[*n*], the stability of the CB[*n*]/MLP complexes are lower than that of the bare CB[*n*]s, whereas the chemical reactivity of the CB[*n*]/MLP complexes are higher than the bare CB[*n*]s. In addition, it is also found that CB[*n*]s are changed in their electrical conductivity due to molnupiravir complexation.

Partial charge transfer (PCT) and host–guest interaction between molnupiravir and CB[*n*] complexation can be interpreted by the NBO (natural bond orbital) analysis [33]. The PCT was defined as $Q_{\mathrm{CB}[n]/\mathrm{MLP}}$–$Q_{\mathrm{MLP}}$, where the $Q_{\mathrm{CB}[n]/\mathrm{MLP}}$ is the total charge of molnupiravir complexation with CB[*n*], and the Q_{MLP} is the charge of isolated molnupiravir. Considering the PCT of molnupiravir complexation, the negative value of PCT denotes the electron transfer from CB[*n*] to molnupiravir molecule; positive PCT value means the opposite process. The computed PCTs of CB[*n*]/MLP complexes are in the range of − 0.004 to − 0.057 *e*. The computed PCT results approve that the charge transfer arises from the CB[*n*] s to the molnupiravir. This indicates that when the CB[*n*] molecules interact with molnupiravir, their charge distributions are altered.

The orbital distributions were computed to analyze electronic property variation of CB[*n*]s corresponding to the complexation with molnupiravir drug. The HOMO and the LUMO distributions of the CB[5]–CB[8], and their complexes with molnupiravir were plotted and displayed in Figs. 6, 7. For the bare CB[*n*]s, all of the HOMO and the LUMO orbitals demonstrate charge delocalization on the CB[*n*]s. Whereas, all of the HOMO and the LUMO orbitals of CB[*n*]/MLP complexes are delocalized on molnupiravir drug. This indicates that after the bare CB[*n*]s complexed with molnupiravir drug, their HOMO and the LUMO orbitals are clearly redistributed. These support the significant modifications in the electronic structures of CB[*n*]s by molnupiravir complexation. In addition, it is found that before and after complexation, the HOMO and LUMO orbitals of CB[*n*]/MLP complexes are located mainly on the molnupiravir drug, (Fig. 2), indicating that the complexation does not alter the electronic nature the of molnupiravir drug and the

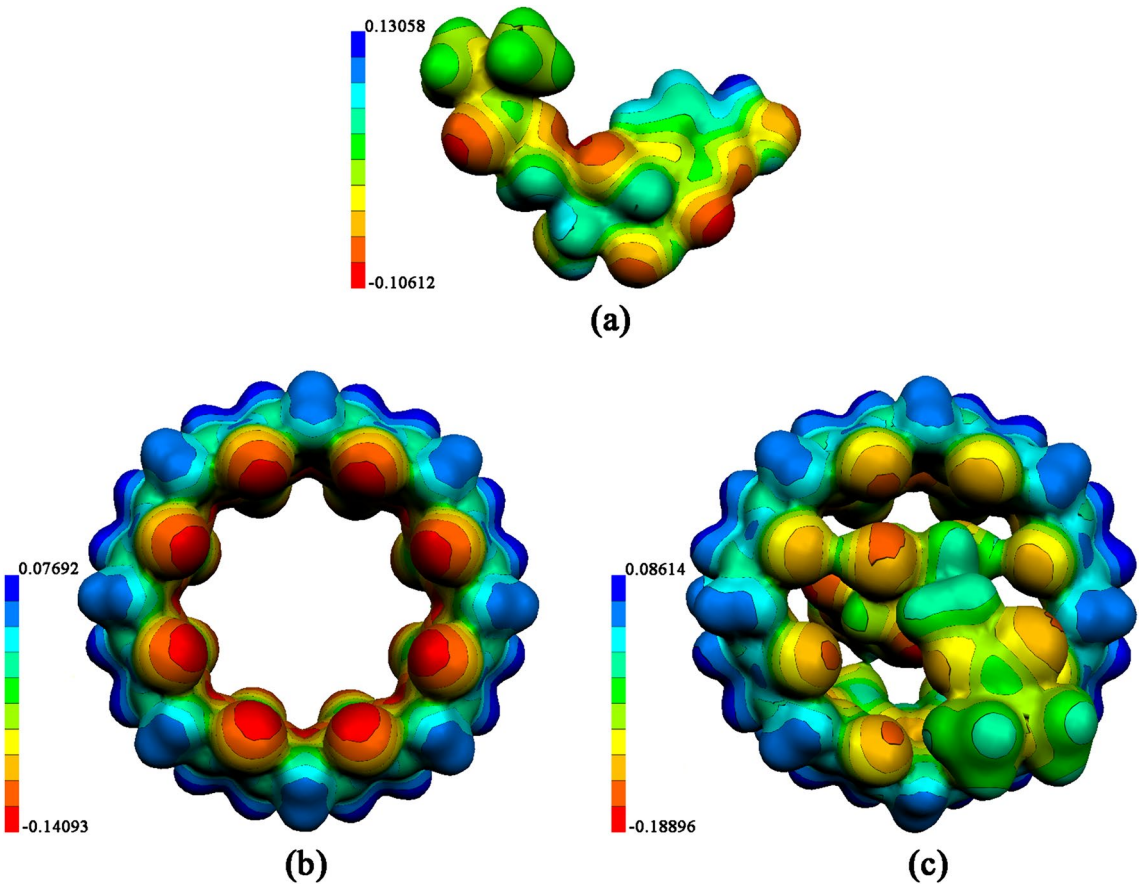

Fig. 9 Computed molecular electrostatic potentials on the molecular surfaces of **a** MLP, **b** CB[8] and, **c** CB[8]/MLP–2. Blue regions are more positive charges and red regions are more negative charge

host–guest interaction occurs by pure physical inclussion [34].

The chemical reactivities of molecules are also related with their electrostatic potentials and hence, the molecular electrostatic potentials (MEP) have been extensively used to identify electrophilic and nucleophilic areas of molecules in electrostatic interactions. The MEP surfaces are defined based on electron density and represented by a RGB color model, in which red regions are more negative charge and blue regions are more positive charge. It is predictable that during the complexation process, the noticed positive region in a compound can interact with any negative region of the other compound, giving rise to a directional interaction [35]. Hence, there can be an increase or decrease in the positive or negative values for the studied inclusion complexes. The MEP contours of bare CB[*n*]s are displayed in Fig. 8, the result show that the negative charges are localized over the portal oxygen atom of CB[*n*]s. The MEP contours of molnupiravir drug, CB[8], and the most stable CB[8]/MLP–2 complex are displayed in Fig. 9. Based on Fig. 9, it is clearly seen that the negative charges are localized over the portal oxygen atoms of CB[8]. After the CB[8] complexed with molnupiravir, the red regions of portal oxygen atom of CB[8] are decreased. Suggesting that the charge transfer occurs from the CB[8] to the molnupiravir molecule which corresponds to the negative PCT values approving the host–guest, molnupiravir–CB[*n*] complex formation.

Conclusions

The DFT optimized geometrical structures of cucurbit[*n*] urils with $n = 5–8$ are found to possess a D_{nh} symmetry. The host–guest complex formation of CB[*n*]–MLP are appropriate in CB[*n*] cavity, except for CB[5]/MLP–1 and CB[5]/MLP–2 complexes, molnupiravir drug is expelled out of the cavity. The intermolecular non-covalent interactions which are the hydrogen bonds between the portal oxygen atom of CB[*n*] and the O−H or N−H of molnupiravir drug are found to play positive role in the CB[*n*]/MLP complex formation. The negative complexation energy values of CB[*n*]/MLP complexes initiated in both gas and water phases are specified that the most host–guest complexes are occurred via an exothermic procedure. In

addition, the CB[8]/MLP–2 complex is more stable than that of all studied CB[*n*]/MLP complexes. Affording to the computed NBO and MEP results, it is indicated that the intermolecular hydrogen interactions in CB[n]/MLP host–guest complexes play an important role with regard to the complexation stability. Furthermore, after molnupiravir complexation, the HOMO and LUMO orbitals and the energy gaps of CB[*n*] are also clearly modified. It can be summarized here that CB[*n*]s can act as a host for appropriately molnupiravir guest, even in aqueous phase. These results can be applied for the design and synthesis of encapsulated drug with cucurbit[*n*]urils.

Author contributions W. Rakrai and B. Wanno contributed to the study conception and design. The DFT calculations were performed by W. Rakrai, C. Tabtimsai, and B. Wanno. The data analysis and the first draft of the manuscript were made by W. Rakrai, and B. Wanno. Revising the manuscript critically for important intellectual content on subsequent versions of the manuscript has done by W. Rakrai, B. Rattanadon, C. Tabtimsai, C. Kaewtong, and B. Wanno. All the authors read and approved the final manuscript.

Funding This research project was financially supported by Thailand Science Research and Innovation (TSRI) 2023, and the Center of Excellence for Innovation in Chemistry (PERCH–CIC), Office of the Higher Education Commission, Ministry of Education, Thailand.

Data availability Not applicable (All data generated or analyzed during this study are included in this published article).

Code availability Not applicable.

Declarations

Competing interests The authors declare no conflicts of interest/competing interests.

Ethics approval The ethical standards have been met.

Consent for publication All co-authors have seen and approved the manuscript.

References

1. Agostini, M.L., et al.: J. Virol. **93**, 24 (2019)
2. Toots, M., Yoon, J.-J., Hart, M., Natchus, M.G., Painter, G.R., Plemper, R.K.: Transl. Res. **218**, 16–28 (2020)
3. Singh, A.K., Singh, A., Singh, R., Misra, A.: Diabetes Metab. Syndr. Clin. Res. Rev.Syndr. : Clin. Res. Rev. **15**, 102329 (2021)
4. Zarenezhad, E., Marzi, M.: Med. Chem. Res. **31**(2), 232–243 (2022)
5. Singh, A.K., Singh, A., Singh, R., Misra, A.: Diabetes Metab. Syndr. Clin. Res. Rev.Syndr. : Clin. Res. Rev. **16**, 102396 (2022)
6. Ezike, T.C., et al.: Heliyon **9**, e17488 (2023)
7. Sahu, K.M., Patra, S., Swain, S.K.: Int. J. Biol. Macromol. **240**, 124338 (2023)
8. Lindoy, L.F., Atkinson, I.M.: Self-assembly in Supramolecular Systems. The Royal Society of Chemistry, Cambridege (2000)
9. Kolesnichenko, I.V., Anslyn, E.V.: Chem. Soc. Rev. **46**, 2385–2390 (2017)
10. Schneider, H.J.: Angew. Chem. Int. Ed. **48**, 3924–3977 (2009)
11. Wang, L., Li, L.L., Fan, Y.S., Wang, H.: Adv. Mater. **25**, 3888–3898 (2013)
12. Macartney, D.H.: Isr. J. Chem. **51**, 600–615 (2011)
13. Jansen, K., Buschmann, H.-J., Wego, A., Döpp, D., Mayer, C., Drexler, H.-J., Holdt, H.-J., Schollmeyer, E.: J. Incl. Phenom. Macrocycl. Chem.Macrocycl. Chem. **39**, 357–363 (2001)
14. Jeon, W.S., Moon, K., Park, S.H., Chun, H., Ko, Y.H., Lee, J.Y., Lee, E.S., Samal, S., Selvapalam, N., Rekharsky, M.V., Sindelar, V., Sobransingh, D., Inoue, Y., Kaifer, A.E., Kim, K.: J. Am. Chem. Soc. **127**, 12984–12989 (2005)
15. Hu, Q.D., Tang, G.P., Chu, P.K.: Acc. Chem. Res. **47**, 2017–2025 (2014)
16. Barrow, S.J., Kasera, S., Rowland, M.J., del Barrio, J., Scherman, O.A.: Chem. Rev. **115**, 12320–12406 (2015)
17. Lagona, J., Mukhopadhyay, P., Chakrabarti, S., Isaacs, L.: Angew. Chemie Int. Ed. **44**, 4844–4870 (2005)
18. Kim, J., Jung, I.S., Kim, S.Y., Lee, E., Kang, J.K., Sakamoto, S., Yamaguchi, K., Kim, K.: J. Am. Chem. Soc. **122**, 540–541 (2000)
19. Sabet, M., Ganji, M.D.: J. Mol. Model. **19**, 4013–4023 (2013)
20. Sin, K.-R., Kim, C.-J., Ko, S.-G., Pak, S.-H., Son, M.-H., Choe, M.-I.: Monatsh. Chem. **152**, 209–216 (2021)
21. Rakrai, W., Tabtimsai, C., Kaewtong, C., Wanno, B.: Struct. Chem. **33**, 757–768 (2022)
22. Venkataramanan, N.S., Suvitha, A., Sahara, R., Kawazoe, Y.: Struct. Chem. **34**, 1869–1882 (2023)
23. Becke, A.D.: Phys. Rev. A **38**, 3098–3100 (1988)
24. Becke, A.D.: J. Chem. Phys. **98**, 5648–5652 (1993)
25. Lee, C., Yang, W., Parr, R.G.: Phys. Rev. B **37**, 785–789 (1988)
26. Frisch, M.J., Trucks, G.W., Schlegel, H.B., Scuseria, G.E., Robb, M.A., Cheeseman, J.R., Scalmani, G., Barone, V., Mennucci, B., Petersson, G.A., Nakatsuji, Caricato, M, Li X., Hratchian, HP., Izmaylov, A.F., Bloino, J., Zheng, G., Sonnenberg, J.L., Hada M., Ehara, M., Toyota, K., Fukuda, R., Hasegawa, J., Ishida, M., Nakajima, T., Honda, Y., Kitao, O., Nakai, H., Vreven, T., Montgomery, J.A., Peralta, JrJ.E., Ogliaro, F., Bearpark, M., Heyd, J.J., Brothers, E., Kudin, K.N., Staroverov, V.N., Kobayashi, R., Normand, J., Raghavachari, K., Rendell, A., Burant, J.C., Iyengar, S.S., Tomasi, J., Cossi, M., Rega, N., Millam, J.M., Klene, M., Knox J.E., Cross, J.B., Bakken, V., Adamo, C., Jaramillo, J., Gomperts, R., Stratmann, R.E., Yazyev, O., Austin, A.J., Cammi, R., Pomelli, C., Ochterski, J.W., Martin, R.L., Morokuma, K., Zakrzewski, V.G., Voth, G.A., Salvador, P., Dannenberg, J.J., Dapprich, S., Daniels, A.D., Farkas, Ö., Foresman, J.B, Ortiz, J.V, Cioslowski J, Fox, D.J (2009) GAUSSIAN 09, Revision A.02, Gaussian Inc, Wallingford CT
27. Barone, V., Cossi, M., Tomasi, J.: J. Comput. Chem. **19**, 404–417 (1998)
28. Cossi, M., Barone, V.: J. Chem. Phys. **109**, 6246–6254 (1998)
29. Flükiger, P., Lüthi, H.P., Portmann, S (2000) MOLEKEL 4.3, Swiss center for scientific computing, Manno, Switzerland
30. Venkataramanan, N.S., Suvitha, A., Sahara, R.: Comput. Theor. Chem. **1148**, 44–54 (2019)
31. Grishaeva, T.N., Masliy, A.N., Kuznetsov, A.M.: J. Incl. Pheom. Marocycl. Chem. **89**, 299–313 (2017)
32. Masliy, A.N., Grishaeva, T.N., Kuznetsov, A.M.: Int. J. Quantum Chem. **119**, e25877 (2018)
33. Glendening, E.D., Landis, C.R., Weinhold, F.: WIREs Comput. Mol. Sci. **2**, 1–42 (2012)
34. Imane, D., Leila, N., Fatiha, M., Abdelkrim, G., Mouna, C., Ismahan, L., Abdelazize, B., Brahim, H.: J. Mol. Liq. **309**, 113233 (2020)

35. Varadwaj, A., Marques, H.M., Varadwaj, P.R.: Molecules **24**, 379 (2019)